JP Journal of Solids and Structures
Volume …, Issue …, 2008, Pages …
This paper is available online at http://www.pphmj.com

EXPERIMENTAL INVESTIGATION OF INFLATABLE CYLINDRICAL CANTILEVERED BEAMS

Z. H. ZHU[a,*], R. K. SETH[b] and B. M. QUINE[a,b]

[a]Department of Earth and Space Science and Engineering
York University, 4700 Keele Street
Toronto, Ontario, Canada M3J 1P3
e-mail: gzhu@yorku.ca

[b]Department of Physics and Astronomy
York University, 4700 Keele Street
Toronto, Ontario, Canada M3J 1P3

Abstract

This paper investigates experimentally the bending of inflatable cylindrical cantilevered beams made of modern fabric materials. A dimensionless form of load vs deflection has been developed to characterize and generalize the bending behavior of the inflatable cylindrical cantilevered beams of different sizes, materials, and inflation pressures in a unified way for easy application. The dimensionless form of experimental results demonstrates that the inflatable beams, highly or lightly inflated, can be modeled by the Euler beam theory accurately before wrinkle occurs. The initial wrinkle is hardly noticeable in the experiments and the transition from non-wrinkle to wrinkle is mainly defined by the slope change of load-deflection curve. Compared with the experimental data, the strain-based wrinkle moment provides a lower bound prediction while the stress-based wrinkle moment gives an upper bound prediction. In the post-wrinkle stage, the Euler beam theory using a nonlinear moment-curvature model gives an upper bound estimation of load-deflection relationship while the finite element analysis based on membrane theory gives a lower bound estimation. The actual collapse moment is hard to measure in experiments due to the

Keywords and phrases: inflatable, fabric beam, cylindrical, wrinkle, cantilever.

*Corresponding author

Received April 22, 2008

inflatable beam becomes unstable in the collapsed stage. However, the trends of experimental results show that the stress-based collapse moment gives the upper limit prediction and the strain-based collapse moment does not agree with the experimental data.

1. Introduction

Inflatable beams have been widely used as load-carrying members in space and aerospace applications [5]. These structures are usually made of modern synthetic fabric materials and the inflation air provides structural capacity by pre-tensioning the fabric. Compared with the conventional beams, the inflatable beams offer benefits such as easy to pack and deploy, lightweight, and low costs. However, the inflatable beam structures are easy to deform when subjected external bending loads and even collapse by local buckling (wrinkle) of the fabric wall, especially for the inflatable cantilevered beams. Therefore, the accurate and efficient prediction of the bending moments of wrinkle and collapse of the inflatable beams becomes critical to the application of inflatable beam structures.

Many efforts have been devoted to the development of mechanics of the inflatable cylindrical beams. There are two types of approaches found in the literatures: the beam-type and the membrane/shell-type. Leonard et al. [7] and Comer and Levy [2] studied the inflatable cylindrical cantilevered beams by the Euler beam theory. In their approaches, the cross-section of the inflated beam was assumed unchanged during the deformation and the nonlinear wrinkle behavior of the fabric was accounted for by assuming the compressive stress in the fabric not admissible. Based on these assumptions, the wrinkle moment ($M_W = \pi R^3 p/2$) and the collapse moment ($M_C = \pi R^3 p$) were derived accordingly. Here, R is the radius of the cylindrical beam and p is the inflation pressure, respectively. Main et al. [8, 9] further studied the inflatable cylindrical cantilevered beams with the consideration of the biaxial stress state in the beam fabric due to the combination of pressurization and structural loads. They argued that the wrinkle of the fabric was due to the compressive strain instead of the stress and

consequently derived lower wrinkle and collapse moments such as $M_W = \pi R^3 p(1 - 2\nu)/2$ and $M_C = \pi R^3 p(1 - 2\nu)$, where ν is the Poisson's ratio of the fabric. Noting the above works did not account for the effects of internal pressure and shear deformation of the fabric, Wielgosz and Thomas [13] modeled the inflatable cylindrical beams by considering the pressure as a follower force and using Timoshenko's beam theory to account for the shear deformation of the fabric. Consequently, an inflatable beam element was developed and applied for the analysis of simply supported inflatable cylindrical beam with central load. The numerical results agree with the experimental data quite well. However, their element does not include the wrinkle effect. Recently, Davids and co-workers [3, 4] developed an inflatable beam element by considering the internal pressure through the volume change and the local fabric wrinkle using Stein and Hedgepeth [11] taut and wrinkled criterion. The numerical results agreed with the experimental data of three-point bending test reasonably. Unfortunately, no comparisons between these inflatable beam elements and the experiments of the cantilevered inflated cylindrical beams are available in the literature.

In addition to the beam-type approach, Fichter [6] modeled the inflated cylindrical beams using membrane theory and considered the effect of inflation pressure using the variational approach. Later, Veldman and Vermeeren [12] studied the inflatable beam using thin shell theory and his results agreed with the experimental data of inflatable thin films reasonably. However, the shell theory gives a higher collapse moment than the membrane theory. This indicates that the behaviors of inflatable beams are sensitive to the beam materials and the inflatable fabric beams can perform differently from the inflatable thin film beams because the latter may have bending capacity even at zero inflation pressure. More recently, Yoo et al. [15] implemented Stein and Hedgepeth [11] taut and wrinkled criterion into a membrane element with commercial FE codes and modeled the wrinkle of inflatable cantilevered beams made of thin film. The numerical predictions agree with the experiments. However, their results predicted a higher wrinkling moment than the beam theory although the predicted collapse moment does not exceed the collapse moment derived by the beam theory.

Nevertheless, all the above works show that the inflated beam does not lose load-carrying capacity immediately when the fabric or film wrinkles. Due to inflation pressure, the early stage of wrinkles may not be visible. The wrinkled beam will continue to carry the external load until the whole cross-section is collapsed. However, the difference between the measured collapse moment and the theoretical prediction was as high as 42% observed in experiments [14]. Moreover, the measured wrinkling moment was usually less than the stress-based wrinkle moment derived from the Euler beam theory. However, in some works the winkling moment predicted by finite element method using membrane theory was higher [15].

These existing efforts represent substantial and novel contributions to the field of inflatable beams. However, the differences in the theoretical predictions of the wrinkle and collapse moments based on different approaches/mechanics models and the discrepancies between the theoretical and experimental wrinkle and collapse moments of the inflated beams result in a great uncertainty in the design of the inflatable structures. Meanwhile, the experimental data of the inflatable cylindrical cantilevered beams in the literatures are in raw form and are not easy to compare each other and to be used as guidelines for design work. This motivates the current experimental investigation of the inflatable cylindrical cantilevered fabric beams. Parametric experimental investigations with different internal pressure, lateral loads, and beam lengths were conducted. A dimensionless form of the experimental load-deflection data is introduced to characterize and generalize the load-deflection relationship in a unified way to make the experimental data easy for design application.

The paper consists of five sections. Following this brief introduction in Section 1, the Section 2 presents the mechanics of the inflatable cylindrical beams. Section 3 describes the experimental set up. Section 4 presents the experimental results. The deflections of inflated cylindrical cantilevered beams of different length were measured with different lateral tip loads at different inflation pressures. The data are analyzed and the mechanics of the inflated beam is discussed. Finally, we conclude the paper in Section 5.

2. Mechanics of Inflatable Beams

2.1. Wrinkling and collapse moments of inflatable cylindrical beam

Consider an inflated cylindrical cantilevered beam subject to a lateral tip load. Assume the cross-section of the inflated cylindrical beam unchanged during the deformation. Based on the Euler beam theory and force equilibrium, the axial and hoop stresses in the inflated cylindrical cantilevered beam at the fixed end can be expressed as, if the wall of the inflated beam does not wrinkle,

$$\sigma_{x\_\min} = \frac{pR}{2t} - \frac{FL}{\pi R^2 t}, \qquad \sigma_{x\_\max} = \frac{pR}{2t} + \frac{FL}{\pi R^2 t}, \qquad \sigma_\theta = \frac{pR}{t}, \quad (1)$$

where p is the internal pressure, F is the external load applied transversely at the tip, R, t, and L are the radius, thickness and length of the beam, σ_x and σ_θ are the axial and hoop stresses, respectively.

The Stein and Hedgepeth [11] taut and wrinkled criterion states that:

$$\sigma_2 > 0\text{: taut;} \qquad \varepsilon_1 \le 0\text{: slack;} \qquad \varepsilon_1 > 0 \text{ and } \sigma_2 \le 0\text{: wrinkle,} \quad (2)$$

where σ_1 and σ_2 $(\sigma_1 \ge \sigma_2)$ are principal stresses and ε_1 and ε_2 $(\varepsilon_1 \ge \varepsilon_2)$ are principal strains, respectively. This wrinkle criterion is equivalent to the tension-only assumption for the inflatable beam [2, 7]. For instance, in the inflated cylindrical cantilevered beam, $\varepsilon_1 = \varepsilon_\theta$ and $\sigma_2 = \sigma_{x\_\min}$. When $\sigma_{x\_\min}$ approaches zero as external load increases, the fabric will wrinkle along the circumferential direction as observed in the experiments. Thus, the wrinkle moment of the inflated fabric beam can be derived as

$$\sigma_{x\_\min} = \frac{pR}{2t} - \frac{FL}{\pi R^2 t} = 0 \quad \rightarrow \quad M_W = FL = \frac{\pi p R^3}{2}, \quad (3)$$

where M_W is the wrinkle moment based on the beam theory and stress-based wrinkle criterion. As the applied load increases beyond this critical value, the wrinkling region of the inflated cylindrical beam expands in the axial and circumferential directions. When the wrinkled

region extends completely around the cross-section area, the inflated cylindrical beam collapses and the corresponding collapse moment can be obtained directly as [2]

$$M_C = FL = \pi pR^2 \times R = \pi pR^3. \tag{4}$$

In addition to the stress-based wrinkle criterion, Main et al. [8, 9] argued that the wrinkle of the fabric was due to the compressive strain not admissible in the fabric because the axial strain of the beam becomes compressive prior to the axial stress due to the Poisson's effect, such that

$$\varepsilon_{x\_\min} = \frac{1}{E}(\sigma_{x\_\min} - \nu_{\theta x}\sigma_\theta) = \frac{1}{E}\left(\frac{pR}{2t} - \frac{FL}{\pi R^2 t} - \nu_{\theta x}\frac{pR}{t}\right) = 0, \tag{5}$$

where $\nu_{\theta x}$ is Poisson's ratio of the fabric of the beam. From Eq. (5), the strain-based wrinkle moment is derived as

$$M_{W\_STN} = FL = \frac{\pi pR^3}{2}(1 - 2\nu_{\theta x}). \tag{6}$$

Correspondingly, the strain-based collapse moment is

$$M_{C\_STN} = FL = \pi pR^3(1 - 2\nu_{\theta x}). \tag{7}$$

Note that the strain-based wrinkle and collapse moments are lower than the stress-based ones by a factor of $(1 - 2\nu_{\theta x})$.

In addition, several semi-empirical expressions of collapse moment can also be found in literature. For instance, the NASA [10] recommended a design formula for the collapse moment,

$$M_{C\_\mathrm{NASA}} = 0.8\pi pR^3. \tag{8}$$

2.2. Normalization of experimental data

In order to get generic information from the experimental results, the dimensionless load m and tip deflections δ are introduced as

$$m = \frac{FL}{\pi pR^3}; \qquad \delta = \frac{Etd}{pL^2}, \tag{9}$$

where E, L, R, t are the Young's modulus, length, radius, thickness of beam, p is the inflation pressure, F is the transverse tip load and d is the transverse tip deflection of beam, respectively.

With Eq. (9), the dimensionless wrinkle and collapse moments can be expressed as,

Wrinkle moment:

Stress-based: $m_W = 0.5$

Strain-based: $m_{W\_STN} = 0.5(1 - 2\nu_{\theta x})$. (10)

Collapse moment:

Stress-based: $m_C = 1.0$

Strain-based: $m_{C\_STN} = 1 - 2\nu_{\theta x}$

NASA [10]: $m_{C\_NASA} = 0.8$. (11)

Accordingly, the tip load-deflection relationship predicted by the Euler beam theory can be expressed dimensionlessly, such that

$$d = \frac{FL^3}{3E\pi R^3 t} \qquad \rightarrow \qquad \delta = \frac{m}{3}. \tag{12}$$

3. Experimental Set Up

The experimental set up is shown in Figure 1. The experiment involves an inflatable cylindrical cantilevered beam made of fiber reinforced polyethylene hose (commercial available, vinylflow general purpose lay flat hose), an air compressor with regulated air supply (2 HP, 8 Gallon, Horizontal Compressor), two air pressure gauges and a loading fixture. The inflatable beam was placed vertically with the lower end of the beam being firmly clamped to an aluminum plug that is rigidly bolted to a heavy base with the air supply. The hose was firstly glued to the aluminum plug with epoxy and then clamped tightly by two hose clamps, see Figure 1(b). The upper end of the beam is closed by another aluminum plug in the same procedure. The mass of the upper plug is $m = 0.685$ kg. An air pressure gauge is mounted on the upper plug to observe the inflation pressure more precisely instead of the pressure

reading at the air compressor. The beam was inflated with air up to a certain level using the regulated air supply. At the upper free end of the beam, the lateral load is applied using a long string (greater than 1.5 times the beam length) and pulley arrangement. The pulley is positioned at the same height relative to the free end to ensure that the applied load will be perpendicular to the beam. A pointer is attached to the weight hanger on the other end of the string to record the deflection on a vertical scale. The transverse deflection of the upper free end is measured at each applied load immediately after the load is applied in order to minimize the creeping effect. The load was then removed and the beam returned to a position slightly off its undeformed position due to the hysteresis of the fabric. The residual deflection of the inflatable fabric beam was about 5% of the total deflection under load. The beam was manually restored to its undeformed position and then next load was applied again. The experiments were conducted at the following inflation pressures: 69 kPa (10 psi), 103 kPa (15 psi), 138 kPa (20 psi), 172 kPa (25 psi), 207 kPa (30 psi) and 241 kPa (35 psi). The accuracy of length and deflection measurement is 0.5 mm, while the accuracy for the pressure and load measure is 7 kPa (1 psi) and 0.01 N, respectively.

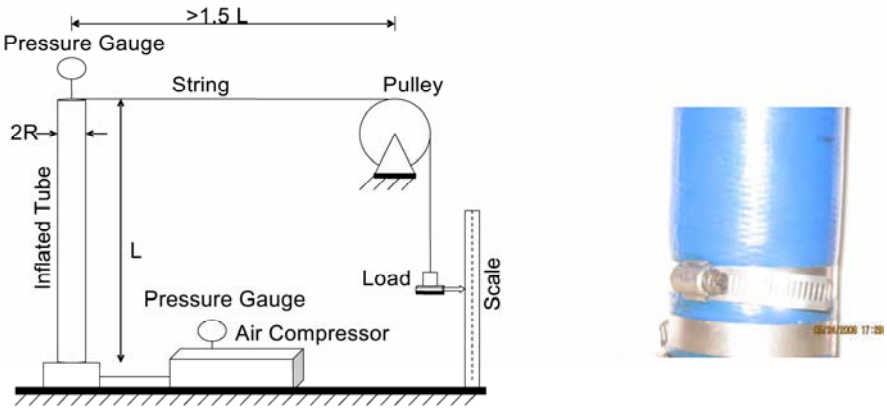

Figure 1. Schematic of experimental set up: (a) system layout, (b) end of inflatable beam.

4. Experimental Results

4.1. Mechanical and geometric parameters of inflatable beams

The mechanical and geometric parameters of the inflatable beam are obtained experimentally. The thickness of the beam is uneven in the length and circumferential directions. It ranges from 1.0 mm to 1.9 mm. An average thickness, t = 1.22 mm, is used in the data post-processing. The averaged inflated radius of the beam is R = 0.041 m. The Young's modulus and Poisson's ratio of the beam fabric were measured by tensile tests as per ASTM D638-03 [1]. The measurements are shown in Table 1. Five samples were die cut into type C samples as per ASTM D638-03 from the beam in the axial and circumferential directions respectively and tested at a pull speed of 5 millimeters per minute.

Table 1. Tensile test results of beam fabric

Test No.	Axial Direction		Circumferential Direction	
	Young's Modulus E_x (MPa)	Poisson's Ratio $\nu_{x\theta}$	Young's Modulus E_θ (MPa)	Poisson's Ratio $\nu_{\theta x}$
1	229.5	0.15	214.8	0.16
2	289.3	0.13	211.8	0.11
3	343.7	0.17	250.5	0.16
4	313.3	0.20	267.4	0.12
5	209.5	0.14	243.1	0.14
Average	277.1	0.16	242.9	0.14

4.2. Load-deflection results of inflated cylindrical cantilevered beam

The bending experiments of the cantilevered beam were conducted using two beam samples of different lengths, namely, $L1$ = 1.484 m and $L2$ = 0.983 m. The ratios of length to diameter of the beams are $L1/(2R) \approx 18$ and $L2/(2R) \approx 12$ and satisfy the requirement of the Euler beam theory. The transverse tip deflections of the inflated beams of different lengths were measured at the different loads and inflation

pressures. The results are shown in Figures 3-4. Clearly, the load capacity of the inflated beam is proportional to the inflation pressure as expected. The load-deflection relationships were linear when the load was low. It is interesting to note that all the linear parts of load-deflection curves of different inflation pressure have the same slope. This suggests that the unwrinkled inflatable beams could be modeled with the Euler beam theory. As the load increased, the load-deflection relationships became nonlinear due to the wrinkle of the fabric and eventually the beam approached to the collapse state. The collapse loads were not obtainable in the experiments because the beam started to pivot at the cantilevered point before reaching the stress-based theoretical collapse load. It was observed in the experiments that the maximum loads obtained before the beam became unstable corresponding to the situation where approximately half of the hose wrinkled as shown in Figure 2.

Figure 2. Wrinkled fabric beam.

The raw experimental data of two beams shown in Figures 3-4 are not very useful in terms of characterizing and generalizing the bending of the inflatable fabric beams. They were further processed into a dimensionless load-deflection form and are shown in Figure 5. As comparison, the load-deflection relationship of the Euler beam theory in Eq. (12) is also shown in Figure 5 together with the wrinkle and collapse moments in Eqs. (10-11) and the post-wrinkle solution of Comer and Levy [2]. The dimensionless experimental data in Figure 5 clearly demonstrate

that the dimensionless m-δ relationship may be approximately fit into a single curve. Compared with the Euler theory, the deflection δ is linearly dependant on the external load m and agrees very well with the Euler theory up to $m \approx 0.4$. Beyond that value, the m-δ relationship gradually becomes nonlinear due to the wrinkle of beam fabric until the external load m approaches the theoretical collapse moment of beam theory $m_C = 1$. In this post-wrinkle stage, the solution based on the Euler beam theory with nonlinear moment-curvature model [2] gives an upper bound of the load capacity of the partially wrinkled inflatable beam. This is partially because the Comer and Levy's nonlinear moment-curvature model neglected the cross-section ovalization of the wrinkled beam. The limit of linear region is halfway between the predictions of strain-based wrinkle moment $(m_{W\_STN} = (1 - 2 \times 0.14)/2 = 0.36)$ and stress-based wrinkle moment $(m_W = 0.5)$. The transition from linear region to wrinkle is gradual. This was evident in the experiments that the noticeable wrinkles of the fabric usually occurred at $m = 0.6$, which exceeds the highest theoretical prediction of wrinkle moment $m_W = 0.5$ although the slope of load-deflection curve starts to change at $m \approx 0.4$.

As the load increases beyond $m = 0.5$, the measured load-deflection relationship becomes highly nonlinear. The measured near collapse moments vary between $0.9\pi pR^3$ and $1.0\pi pR^3$ or $0.9 \le m \le 1.0$. These results support the stress-based theoretical collapse moment $M_C = \pi pR^3 (m_C = 1)$ should be the upper limit of the actual collapse moment of an inflatable beam. It also seems that the collapse moment suggested by NASA [10] give a conservative lower bound for design application. The strain-based collapse moment prediction does not agree with the experimental results.

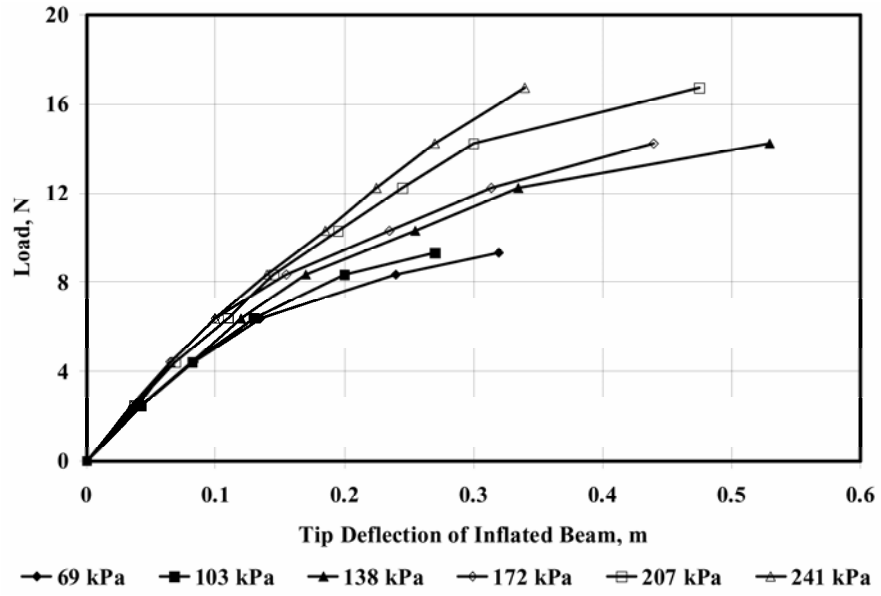

Figure 3. Experimental load-deflection curves of inflated beam L1.

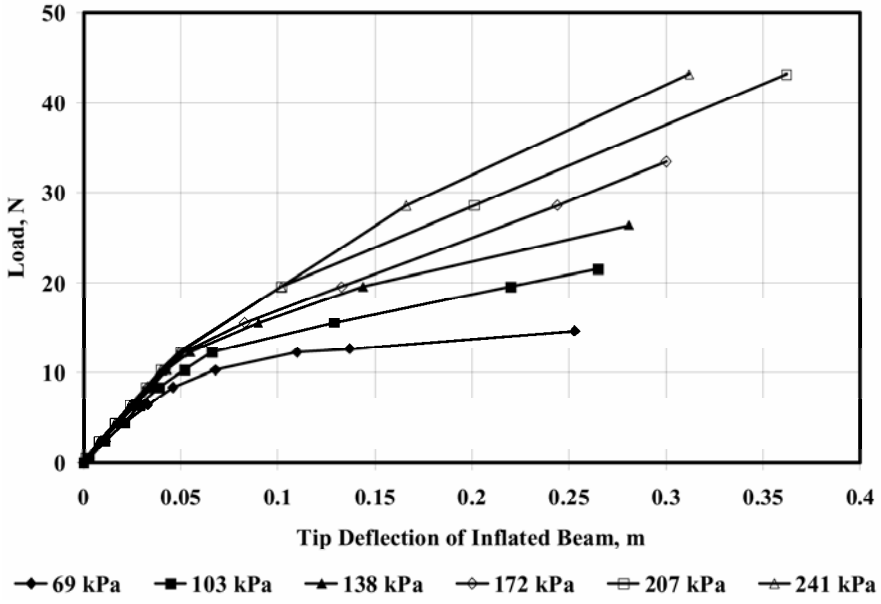

Figure 4. Experimental load-deflection curves of inflated beam L2.

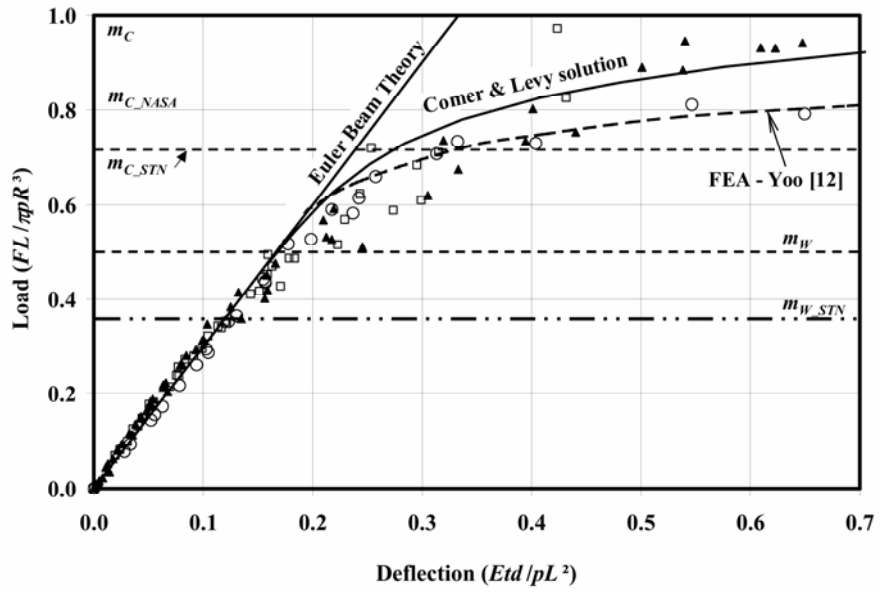

Figure 5. Comparison of experimental, analytical and FEM dimensionless load-deflection relationships: □ - Beam L1, ▲ - Beam L2, ○ - Exp. - Yoo [15].

In addition, this dimensionless procedure has been applied to the experimental results and finite element predictions reported by Yoo et al. [15] and compared with current experimental data in Figure 5. In their work, an inflatable cylindrical cantilevered beam made of thin film subjected to low inflation pressure ($p_{\max}$ = 6.9 kPa compared with the current experiments $p_{\min}$ = 69 kPa) was modeled with the membrane elements and tested. Their FEM and experimental results agree reasonably well with the current experimental data of inflatable fabric beams in the dimensionless load-deflection form, showing that the dimensionless load-deflection form can be used to reveal the common characteristics of the inflatable beams made of different materials and working in different conditions. Interestingly, the FEM solution [15] gives an unusual higher wrinkle moment ($m = 0.6 > m_W = 0.5$) although the corresponding experimental data in [15] shows the wrinkle occurs at $m = 0.5$ approximately. This is hard to explain. It may be due to the

residual bending stiffness of the thin film beam at zero pressure, which is different from the fabric beam that has no banding stiffness at zero pressure. The comparisons also show that the FEM solution predicts a lower bound of load capacity in the post-wrinkle stage of the inflatable beam compared with the theoretical solution of Comer and Levy [2]. This may be because the membrane finite element solution accounts for the cross-section ovalization effect of the inflatable beam, which is neglected by the Euler beam theory.

5. Conclusion

Experimental investigation of inflatable cylindrical cantilevered fabric beams has been conducted in order to obtain design guidelines for the inflated cylindrical beam structures. A dimensionless form of load-deflection relationship has been used to characterize and generalize the behavior of inflatable cylindrical cantilevered fabric beams of different sizes and different inflation pressures in a unified way for easy application. The experimental results indicate that the wrinkle of the inflated fabric beam occurs because the fabric cannot resist compression. The current and previous [15] experimental results show that the inflatable beam, either highly or lightly inflated, can be modeled by the simple Euler beam theory accurately before the wrinkle occurs. The initial wrinkle is hardly noticeable in the experiments and the transition from non-wrinkle to wrinkle occurs gradually. The critical point of wrinkle is determined mainly by monitoring the slope change of load-deflection curve. Compared with the dimensionless experimental data, the strain-based wrinkle moment gives a lower bound estimation while the stress-based wrinkle moment gives an upper bound estimation. In the post-wrinkle stage, the Euler beam theory with the nonlinear moment-curvature model gives an upper bound estimation of the load-deflection relationship while the finite element analysis [15] based on the membrane theory gives a lower bound estimation. The difference between the two approaches is mainly because the beam-type approach assumes the cross-section of beam undeformed in bending while the FEM approach has no such restriction. The actual collapse moment is hard to

measure in the experiments due to the inflatable beam becoming unstable near the collapsed stage. However, the trends of experimental results show that the stress-based collapse moment is the upper limit and the strain-based collapse moment does not agree with the experimental data.

In conclusion, the current experimental investigations demonstrate that the bending of inflatable cylindrical beam can be modeled simply using the Euler beam theory before the beam starts to wrinkle. In the post-wrinkle stage, the Euler beam theory using the nonlinear moment-curvature model of Comer and Levy [2] can provide a reasonable estimation of the wrinkled bending behavior of the inflatable beam. The dimensionless form of load-deflection data provides a good tool to reveal some common characteristics of inflatable beams made of different materials with different sizes and working in different conditions.

References

[1] ASTM Standard D638-03, Standard Test Method for Tensile Properties of Plastics, ASTM International, West Conshohocken, PA, USA, 2003.

[2] R. L. Comer and S. Levy, Deflections of inflated circular cylindrical cantilever beam, AIAA J. 1 (1963), 1652-1655.

[3] W. G. Davids et. al., Beam finite-element analysis of pressurized fabric tubes, J. Struct. Eng.-ASCE 133 (2007), 990-998.

[4] W. G. Davids, Finite-element analysis of tubular fabric beams including pressure effects and local fabric wrinkling, Finite Elem. Anal. Des. 44 (2007), 24-33.

[5] H. F. Fang, M. Lou and J. Huang et al., Inflatable structure for a three-meter reflectarray antenna, J. Spacecraft Rockets 41 (2004), 543-550.

[6] W. B. Fichter, A theory for inflated thin-wall cylindrical beams, NASA TN D-3466, 1966.

[7] R. W. Leonard, G. W. Brooks and H. G. McComb, Jr., Structural considerations of inflatable reentry vehicles, NASA TN D-457, Virginia, USA., 1960.

[8] J. A. Main, S. W. Peterson and A. M. Strauss, Load-deflection behavior of space-based inflatable fabric beams, J. Aerospace Eng. 2 (1994), 225-238.

[9] J. A. Main, S. W. Peterson and A. M. Strauss, Beam-type bending of space-based inflated membrane structures, J. Aerospace Eng. 8 (1995), 120-125.

[10] NASA Space Vehicle Design Criteria, Buckling of Thin-Walled Circular Cylinders, NASA SP-8007, 1968.

[11] H. Stein and J. M. Hedgepeth, Analysis of partly wrinkled membranes, NASA TN D-813, 1961.

[12] S. L. Veldman and C. A. Vermeeren, Jr., Inflatable structures in aerospace engineering-an overview, Proceedings of the European conference on spacecraft structures, materials and mechanical testing, Noordwijk, The Netherlands, ESA SP 468, 2000, pp. 93-98.

[13] C. Wielgosz and J. C. Thomas, Deflections of highly inflated fabric tubes, Thin-Walled Structures 42 (2004), 1049-1066.

[14] C. Wielgosz, T. C. Thomas and P. Casari, Strength of inflatable fabric beams at high pressure, 43rd AIAA/ASME/ASCE/AHS Structures, Structural Dynamics and Materials Conference, AIAA 2002-1292, Denver, Colorado, USA, 2002.

[15] E.-J. Yoo et. al., Wrinkling control of inflatable booms using shape memory alloy wires, Smart Mater. Struct. 16 (2007), 340-348.